# Structure of an inert layer of 4He adsorbed on mesoporous silica



doi: 10.1103/PhysRevB.100.024103

# Structure of an inert layer of $^4$He adsorbed on mesoporous silica

Junko Taniguchi,* Kizashi Mikami, and Masaru Suzuki
*Department of Engineering Science, University of Electro-Communications, Chofu, Tokyo 182-8585, Japan*

(Received 8 April 2019; revised manuscript received 17 June 2019; published 3 July 2019)

We have performed the measurements of the vapor pressure and heat capacity for inert layer $^4$He adsorbed on a mesoporous silica. The heat capacity was found to exhibit a Schottky peak, indicating the excitation of the localized solid to fluid. We analyzed the heat capacity over a wide temperature range according to a model that considers the contribution of the localized solid and excited fluid, and clarified that the excited fluid coexists with the localized solid at high temperatures. Based on the areal density dependence of the amount of excited fluid, we discuss the formation of an inert layer prior to the appearance of a superfluid layer.

DOI: 10.1103/PhysRevB.100.024103

## I. INTRODUCTION

Since the observation of the Kosterlitz-Thouless transition in a $^4$He film formed on vycor glass [1], a considerable amount of work has been reported on the structure of $^4$He films adsorbed on various substrates. On graphite, which exhibits a homogeneous adsorption potential, layer-by-layer growth of films was confirmed up to six atomic layers [2], and highly complicated phase diagrams have been obtained for the first and second layers [3,4]. Such complicated phase diagrams have not been reported for other substrates because of their heterogeneous adsorption potential. On these substrates, it is thought that an inert layer is formed at areal densities below the value at which a superfluid layer appears ($n_C$).

Among various heterogeneous substrates, the film structure on a porous vycor glass has been thoroughly studied on the basis of heat capacity measurements [5]. Tait and Reppy attributed the observed bend in heat capacity to the excitation of a part of $^4$He from localized solid islands to delocalized gas areas. They reported that, on the high temperature side of the bend, the excited gas coexists with solid islands and covers only a fraction of the total surface area, owing to the lateral pressure caused by the long-range variation of adsorption potential.

Recently, Toda *et al.* studied the film structure of $^4$He adsorbed on hybrid mesoporous materials (HMM) based on vapor pressure and heat capacity measurements [6]. They observed a heat capacity similar to that for an inert layer and proposed at areal densities above the value for the completion of the first layer, the heat capacity on the high-temperature side of the bend corresponds to that of a normal fluid with an amorphous-solid-like temperature dependence [7]. In order to confirm this hypothesis, they first qualitatively evaluated the density states of two-level systems (TLSs) in the amorphous solid state using the vapor pressure data.

In the previous work, the structure of the inert layer was discussed on the basis of the heat capacity of limited temperature or areal density regions. In this work, our aim is to comprehensively and quantitatively study this structure. Thus, we chose the mesoporous silica called folded-sheets-mesoporous materials (FSM), whose adsorption potential has been theoretically studied [8], and performed heat capacity and vapor pressure measurements. We analyzed the heat capacity of the inert layer over a wide temperature range (0.18–4.5 K) according to a model that considers the contribution of localized solid and excited fluid. The results support the conjecture that the excited fluid coexists with the localized solid at high temperatures. On the other hand, the amount of excited fluid tends to zero as the areal density approaches $n_C$, suggesting a new possibility that the inert layer is solidified at values immediately below $n_C$.

## II. EXPERIMENTS

The synthesis of FSM was first reported by Inagaki *et al.* at Toyota Central R&D Labs., Inc. Japan [9]. This material exhibits a honeycomb structure of straight one-dimensional (1D) uniform nanometer-sized channels without interconnections. Using an organic molecule as a template, the diameter of the channel was precisely controlled, and the homogeneity was confirmed by transmission electron micrography and x-ray diffraction (XRD) [10]. The sample used in this work has channels with a diameter of 2.8 nm and is formed into pellets by mixing it with silver powder.

For heat capacity measurements, we used the cell described in previous heat capacity measurements for pressurized liquid $^4$He [11]. The surface area ($S$) was reduced to 145 m$^2$ in the present measurements, by 20% from the previous one [12]. Unlike in the liquid case, the filling capillary is directly connected to the cell since the thermal conductivity is not excessively high.

The heat capacity was measured using a quasiadiabatic heat-pulse technique at up to 14 atoms/nm$^2$, which corresponds to the areal density of superfluid onset ($n_C$) [13]. The temperature of the cell was monitored with $RuO_2$, which was attached to the bottom face of the cell. This thermometer was calibrated against a calibrated $RuO_2$ thermometer. The thermal relaxation time from the cell to the stage was

*tany@phys.uec.ac.jp

 

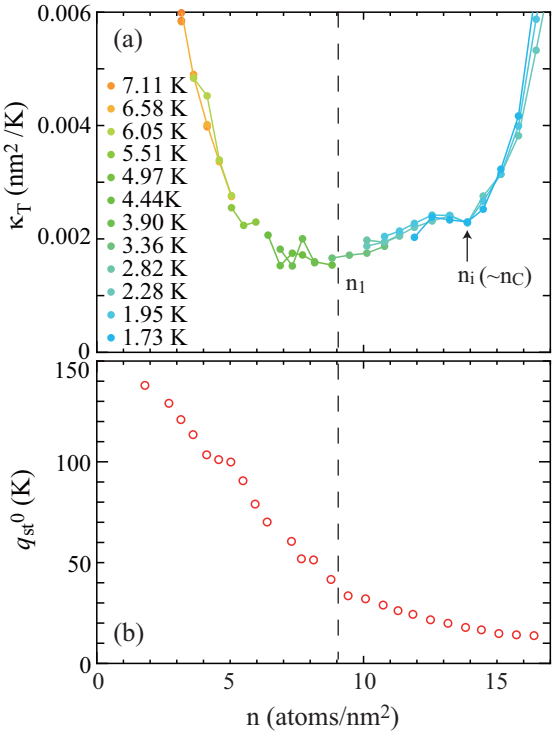


FIG. 1. (a) Two-dimensional isothermal compressibility $\kappa_T$ and (b) isosteric heat of sorption at absolute zero $q_{st}^0$ as a function of areal density. The vertical dashed line shows $n_1$, while the arrow shows $n_i$.

360–5000 s, which is more than one order of magnitude larger than that in the cell, 40–240 s.

For vapor pressure measurements, we adopted the cell described in previous double torsional oscillator measurements [14]. As in previous work [15], the pressure was measured by means of the capacitive strain gauge with a 100 $\mu$m thick membrane, whose one side was Au sputtered as an electrode. The pressure was calibrated against the $^4$He saturated vapor pressure. Its accuracy was $2 \times 10^{-3}$ mbar. This gauge was attached directly to the cell, which was mounted on the 1 K pot of a refrigerator.

## III. RESULTS AND DISCUSSION

### A. Isothermal compressibility and isosteric heat of sorption

The vapor pressure ($P$) of the adsorbed $^4$He determines the isothermal compressibility ($\kappa_T$) and the isosteric heat of sorption ($q_{st}$), which are useful for examining the changes in the film structure. Since $\kappa_T$ decreases as the density increases near layer completion, its minimum is often used to indicate layer completion. $\kappa_T$ is deduced from the $P$ isotherm as

$$\kappa_T = \frac{1}{n^2 k_B T}\left(\frac{\partial n}{\partial \ln P}\right), \tag{1}$$

where $n$ is the areal density, $k_B$ is Boltzmann constant, and $T$ is the temperature.

Figure 1 shows the obtained $\kappa_T$ as a function of areal density up to 16.4 atoms/nm$^2$, where capillary condensation occurs. $\kappa_T$ shows a minimum at approximately $9 \pm 1$ atoms/nm$^2$, which we designate as the areal density of the first layer completion ($n_1$). For values higher than $n_1$, $\kappa_T$ initially increases with increasing areal density and then decreases at approximately $12.7 \pm 0.3$ atoms/nm$^2$, with a slight minimum at $n_i = 14$ atoms/nm$^2$. A similar minimum in $\kappa_T$ was also reported for $^4$He in 4.7- and 2.8-nm channels of FSM series by Ikegami *et al.* [15,16]. Just above the areal density of this slight minimum, a superfluid transition is commonly observed in both the present and the previous work, i.e., $n_C$ almost coincides with $n_i$. This finding indicates that the inert layer is slightly compressed as the areal density approaches $n_C$.

From the temperature dependence of the vapor pressure, we calculated $q_{st}$ as

$$q_{st} = -k_B \frac{d \ln P}{d(1/T)}. \tag{2}$$

By subtracting the heat capacity of gas-phase $^4$He, we estimate the isosteric heat of sorption at absolute zero, $q_{st}^0 = q_{st} - (5/2)k_B T$, which corresponds to the depth of the adsorption potential [6]. The obtained $q_{st}^0$ is shown as a function of $n$ in Fig. 1(b). It is ~140 K at 1.8 atoms/nm$^2$ and decreases monotonously with increasing areal density. It reaches ~40 K at $n_1$, above around which its decrease becomes slow. The obtained value of $q_{st}^0$ is close to that of 4.7-nm channels of FSM, up to $n_1$ [15]. This result indicates that the difference in the channel size between 2.8 and 4.7 nm does not strongly affect the adsorption potential in the submonolayer region.

### B. Heat capacity of inert layer $^4$He

Figure 2 shows the heat capacity ($C$) for various areal densities as a function of $T$. Here the heat capacity of the empty cell is subtracted. Its magnitude is around half of the one of $^4$He at 3.5 atoms/nm$^2$ above 1 K, while it becomes comparable near the lowest temperature. For 3.5 atoms/nm$^2$, a broad peak appears at around 1.1 K, in addition to the slope slightly smaller than $T^2$. With increasing areal density, this peak shifts to the low-temperature side, with its height decreasing. Finally, it becomes unclear above 11.4 atoms/nm$^2$. Since the peak is very broad, we define $T_p$ as the temperature at which $C/T$ begins to deviate from the extrapolation of the low-temperature side, which gives the lower limit of the peak temperature (see the inset of Fig. 2 ). In contrast, the temperature dependence on the high-temperature side remains below $T^2$ up to around 10.2 atoms/nm$^2$, and above that the slope decreases slightly.

As shown in the inset of Fig. 2, the heat capacity above $T_p$ can be explained by the sum of the $T$-linear ($y$-intercept) and $T$-squared (slope) terms. In addition, there is a peak near $T_p$. Notably, the heat capacity near the lowest temperature is lower than the extrapolated value from the high-temperature side of $T_p$ (dashed line in the inset of Fig. 2). The difference for the $T$-linear term may stem from the contribution of the excited atoms near $T_p$.

We set the heat capacity model as

$$C = (A_l T + BT^2) + C_f + D\frac{(\beta\Delta E)^2}{\cosh^2(\beta\Delta E)}, \tag{3}$$

$$C_f = A_f \frac{\exp(-\beta\Delta E)}{\exp(\beta\Delta E) + \exp(-\beta\Delta E)} T, \tag{4}$$

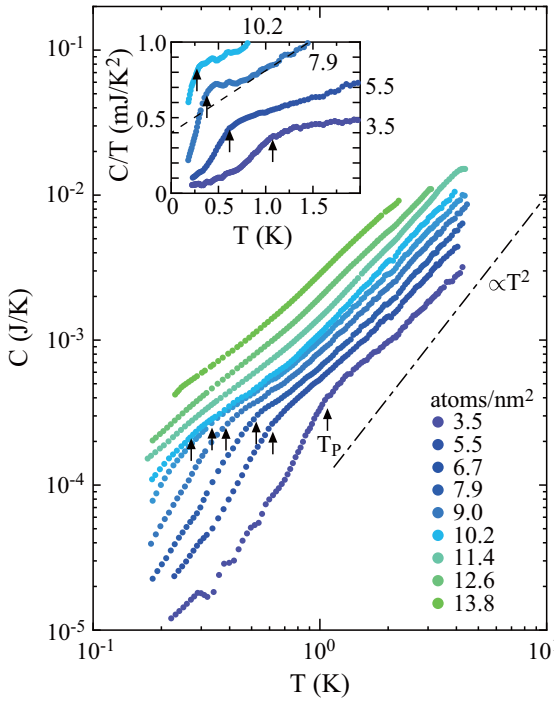


FIG. 2. Heat capacity of $^4$He as a function of temperature for various areal densities below 14 atoms/nm$^2$. The arrows indicate $T_p$, and the dot-dashed line is proportional to $T^2$. The areal densities are presented in units of atoms/nm$^2$. Inset: $C/T$ as a function of $T$ below 10.2 atoms/nm$^2$. The dashed line displays an extrapolation from the high-temperature side of the peak.

where $\beta = 1/k_B T$. Here, the first set of parentheses, the second and third terms correspond to the heat capacity of the localized solid, the two-dimensional (2D) excited-fluid $^4$He, and a Schottky peak due to the excitation, respectively. Regarding their origins, Tait and Reppy suggested that the $A_1 T$ and the $BT^2$ terms arise from the amorphous property and 2D phonon of the localized solid and that $C_f$ from the Bose-gas-like behavior of the excited fluid. $A_f T$ means the heat capacity of the excited fluid at temperatures much higher than $T_P$, and $2\Delta E$ is the energy gap between the localized solid and the 2D fluid states. On the basis of this model, we will evaluate the film structure.

Figure 3(a) shows the fitted curves for 5.5 atoms/nm$^2$ as an example. The heat capacity is well reproduced over the entire temperature range. Near the lowest temperature, the $A_1 T$ term becomes dominant, whereas near the highest temperature the $BT^2$ term is dominant. At around $T_p$, the contribution of the Schottky peak increases, and the coefficient of the $T$-linear term increases because of the contribution of $C_f$. As the areal density is increased, the contribution of the Schottky peak and $C_f$ decreases, as is clear from the heat capacity at 9.0 atoms/nm$^2$ in Fig. 3(b). Further increasing areal density, their contribution disappears, as shown in Fig. 3(c) (13.8 atoms/nm$^2$). The heat capacity for all areal densities between 3.5 and 13.8 atoms/nm$^2$ is fitted well to Eq. (3).

### C. Properties of the localized solid

It is well known that the amorphous property of the localized solid is characterized by the $T$-linear heat capacity due

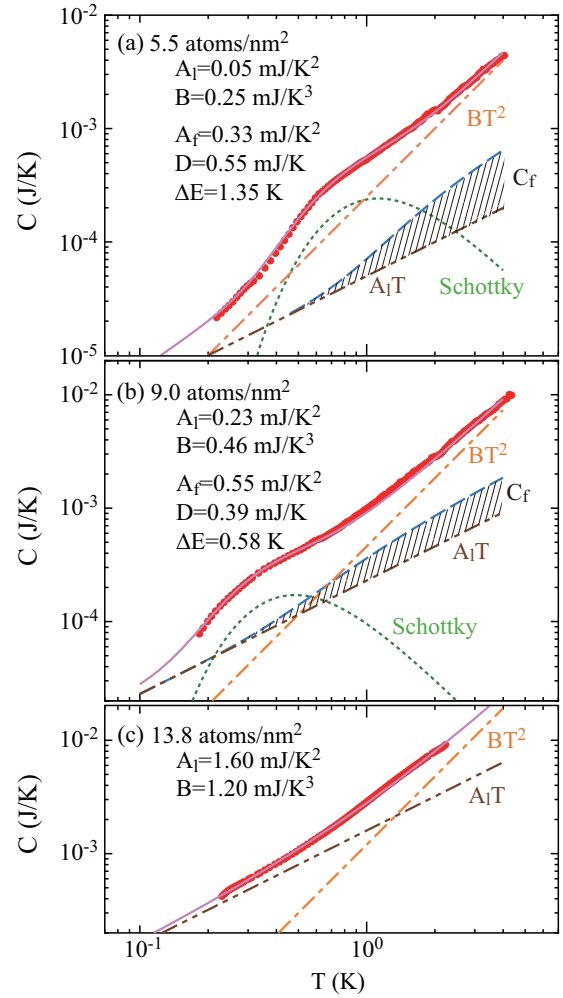


FIG. 3. Heat capacity of $^4$He at (a) 5.5, (b) 9.0, (c) 13.8 atoms/nm$^2$ as a function of temperature. The solid curves are the fitted curves to Eq. (3). The dot-dot-dashed, dot-dashed, and dotted curves correspond to the $A_l T$, $BT^2$, and the Schottky terms in Eq. (3), respectively. The hatched areas correspond to $C_f$.

to quantum tunneling between different states in the two-level systems (TLSs). Figure 4(a) shows the fitting results for $A_l$ as a function of areal density. The values remain small until approximately 9 atoms/nm$^2$ and then increase rapidly with increasing areal density.

The coefficient of the $T$-linear heat capacity for the amorphous solid is described as $A_{aS} = \pi^2/6 \cdot D_0 k_B$, where $D_0$ is the density of states [6]. When the TLS is generated by the adsorption potential distribution, $D_0$ is often approximated as [5,6]

$$D_0 = \left( \frac{\Delta q_{st}^0}{\Delta n} \right)^{-1}. \tag{5}$$

Using $q_{st}^0$ in Fig. 1(b), we estimated $A_{aS}$, which is shown in Fig. 4(a) for comparison. The calculated $A_{aS}$ shows the same areal density dependence as $A_l$, except that the values are slightly larger than $A_l$. This semiquantitative agreement indicates that the $A_l T$ term is well explained by the contribution of amorphous solid.

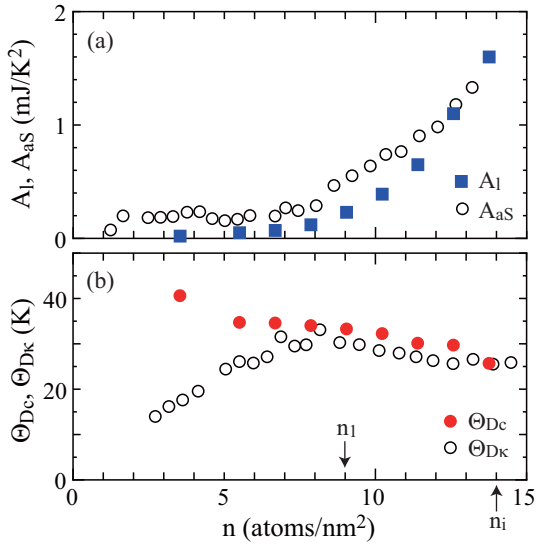


FIG. 4. (a) Fitting results for $A_1$ and the calculated $A_{aS}$ as a function of areal density. (b) Debye temperatures obtained from $B$ ($\Theta_{Dc}$) and $\kappa_T$ ($\Theta_{D\kappa}$) as a function of areal density.

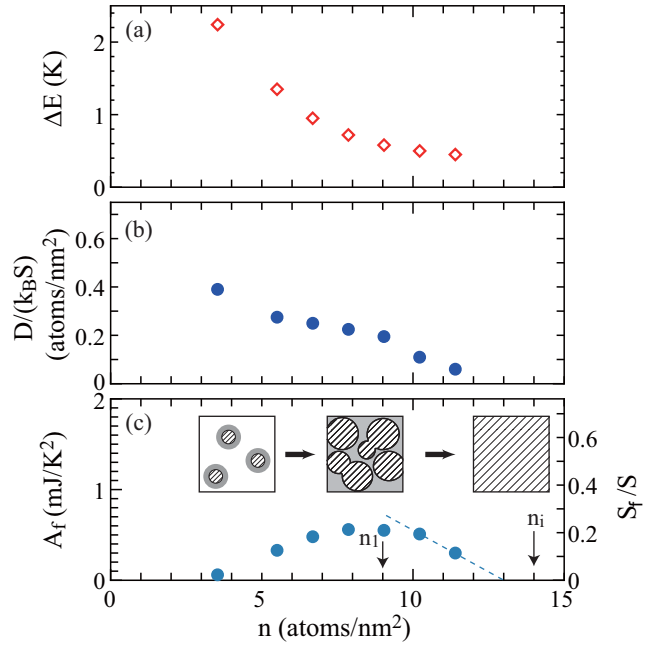


FIG. 5. Fitting results for (a) $\Delta E$, (b) $D/(k_BS)$, and (c) $A_f$ as a function of areal density. In (c), the dashed line shows the extrapolation of the decrease above 10 atoms/nm$^2$. The right vertical axis of (c) is $S_f/S$. The inset plots in (c) show schematic top views of the film at approximately 3.5 atoms/nm$^2$, $n_1$, and $n_i$, from left to right (at $T \gg T_p$ for the former two areal densities). The hatched and gray areas correspond to solid and fluid areas, respectively.

Next, we consider the $BT^2$ term. From the fitting result for $B$, we calculate the effective Debye temperature $\Theta_{Dc}$ as $\Theta_{Dc} = \sqrt{12\zeta(3)\Gamma(3)Nk_B/B} = \sqrt{28.8Nk_B/B}$, where $N$ is the number of solid $^4$He atoms. Here, we approximate $N$ by multiplying $n$ by the surface area $S$, neglecting the number of excited $^4$He atoms. The areal density dependence of $\Theta_{Dc}$ is shown in Fig. 4(b). $\Theta_{Dc}$ is 43 K for 3.5 atoms/nm$^2$ and decreases to ~35 K at 5.5 atoms/nm$^2$, and for higher densities decreases slightly with increasing areal density. The value at around $n_1$ (34 K) is close to those of other substrates such as Ar-plated Cu (32 K) [17] and graphite (33 K) [18].

The Debye temperature can also be deduced from the phonon velocity ($v_p$) as $\Theta_{D\kappa} = (hv_p/k_B)\sqrt{n/\pi}$. The phonon velocity is related to the adiabatic compressibility $\kappa_S$ as $v_p = \sqrt{1/(mn\kappa_S)}$. Here, we evaluate $\Theta_{D\kappa}$ by assuming that $\kappa_T$ is approximately equal to $\kappa_S$ [6]. $\Theta_{D\kappa}$ increases with increasing areal density and then begins to decrease at 8 atoms/nm$^2$, above which $\Theta_{D\kappa}$ agrees well with $\Theta_{Dc}$. It remains unclear why $\Theta_{D\kappa}$ is smaller than $\Theta_{Dc}$ below 8 atoms/nm$^2$. However, it is possible that, in this areal density region, the solid islands are considered to be independent of each other. In this situation, $\kappa_T$ may not reflect the compressibility of the solid $^4$He itself.

The monotonic decrease of $\Theta_{Dc}$ with increasing areal density is not intuitive. Naively, when the areal density increases, the film is expected to be compressed, making the film stiff (i.e., raising the Debye temperature). In fact, for monolayer $^4$He adsorbed on graphite, an increase in the Debye temperature has been reported [18]. In order to understand the monotonic decrease of $\Theta_{Dc}$, it is necessary to consider the fact that the local areal density is not uniform on heterogeneous substrates.

### D. Excitation to the 2D fluid state

First, we focus on the Schottky peak. In Figs. 5(a) and 5(b), $\Delta E$, and $D$ divided by $k_BS$ are plotted as a function of $n$, respectively, for values up to 11.4 atoms/nm$^2$, above which a peak cannot be identified. Here, $D/(k_BS)$ corresponds to the number of atoms that can be excited per unit of areal density. $\Delta E$ is 2.2 K for 3.5 atoms/nm$^2$ and decreases with increasing areal density, at a decreasing rate. The areal density dependence and the order of magnitude of $\Delta E$ agree with those for $^4$He on vycor glass, supporting the view that the adsorbed $^4$He on the present substrate is excited to the fluid state.

On the other hand, $D/(k_BS)$ is at most ~10% for 3.5 atoms/nm$^2$ and decreases with increasing areal density. Above $n_1$, it decreases at an accelerated rate and appears to reach zero at approximately 13 atoms/nm$^2$. The fitting results indicate that the 2D fluid disappears immediately before $n_i$.

In order to examine the relation between the amount of 2D fluid $^4$He and the magnitude of the $T$-linear heat capacity, we plot $A_f$ as a function of $n$ in Fig. 5(c). $A_f$ is 0.06 mJ/K$^2$ for 3.5 atoms/nm$^2$ and initially increases with increasing areal density. It remains almost constant between 8 and 10 atoms/nm$^2$ and then decreases. It is important that $A_f$ is not proportional to $D/k_BS$ [i.e., the amount (areal density) of 2D fluid at high temperatures].

In the case where the excited fluid behaves as an ideal 2D Bose gas, the heat capacity is $T$ linear and depends not on the areal density of the fluid but on the surface area that the fluid covers ($S_f$). The coefficient is expressed by $(mS_f)/(2\pi\hbar^2) \cdot k_B^2$, where $m$ is the mass of the $^4$He atom [19]. When the entire surface area is covered, the coefficient reaches 2.6 mJ/K$^2$, which is much larger than the obtained $A_f$, suggesting

that only a part of the surface is occupied by the excited fluid.

Based on the change in $S_f/S$, we consider the structure of the inert layer. Here, we define $S_f/S$ as $A_f/(2.6\ \mathrm{mJ/K^2})$, which is shown as the right vertical axis of Fig. 5(c). On the other hand, the surface area covered by the localized solid ($S_s$) increases roughly in proportion to $n/n_1$, in the submonolayer region. $S_f$ initially increases in conjunction with $n$ and its increase stops at approximately 8 atoms/nm$^2$, where the sum of $S_f$ and $S_s$ exceeds $S$. The almost constant $S_f$ from 8 to 10 atoms/nm$^2$ indicates that the ratio of localized solid in the first layer increases, while the location of the excited fluid shifts to the overlayer. This trend is thought to be accompanied by the compression of the first layer, since $\kappa_T$ reaches a minimum in the same areal density region. At higher areal densities, $S_f/S$ begins to decrease and tends to zero at approximately 13 atoms/nm$^2$. This behavior is attributed to the increased density in the overlayer, which increases the ratio of solid to fluid in the overlayer and finally enables the solidification of the entire overlayer. This trend is consistent with the decrease in $\kappa_T$ above approximately 13 atoms/nm$^2$, demonstrating that the compression starts at the end of the coexistence of the fluid and solid.

As the origin of the limit for $S_f$, the lateral pressure due to the long-range variation of adsorption potential is suggested [5]. In the case of porous vycor glass, it is thought that the pore size distribution determines the variation of adsorption potential. Although the channel size of FSM is uniform, it has been reported that the adsorption potential of a hexagonal channel has an azimuthal dependence on the cross section [8]. Its amplitude is several tens of Kelvins near the pore wall and decreases as the distance from the wall increases [i.e., as the film thickness (areal density) increases]. The amplitude of variation of the adsorption potential in the submonolayer region is larger than the obtained $\Delta E$, allowing the excited fluid to localize only around the boundaries of the solid islands.

### E. Phase diagram

Here, we evaluate the phase diagram of $^4$He film on the bases of the foregoing discussion. Figure 6 presents $T_P$ and the dissipation peak temperature due to the superfluid in the channel ($T_C$), as a function of areal density. In the low areal density region, $^4$He atoms are adsorbed onto areas with a deep adsorption potential and form solid islands at low temperatures. Near $T_P$, a small part of the localized solid is excited and forms a fluid area surrounding the solid islands. With increasing areal density, $T_P$ decreases because of the decrease in the variation of adsorption potential and finally reaches zero at approximately 13 atoms/nm$^2$. Above this areal density, instead of a decrease in the fluid areas, we observe a compression of the inert layer composed of only solid. Then above $n_i$, a liquid layer which shows superfluidity below $T_C$ appears on top of the inert layer.

This phase diagram is similar to the characteristic diagram of adsorbed $^4$He on porous vycor glass proposed by Tait and

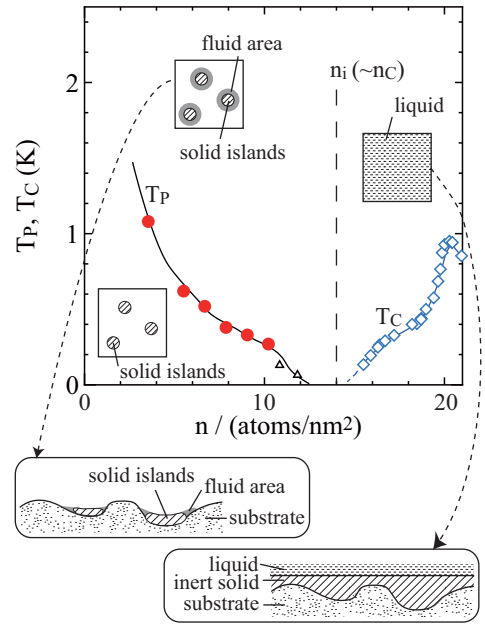


FIG. 6. $T_P$ and the dissipation peak temperature due to the superfluid in the channel ($T_C$) as a function of areal density. The triangles (△) presents $T_P$ from Ref. [20]. The dashed line corresponds to $n_i$, which coincides with $n_C$ experimentally. Inset: Schematic top views of the film near the lowest temperature and slightly above $T_P$ at $n < n_i$, and above $T_C$ at $n > n_i$, from left to right. The two lower left and right panels show cross-sectional images of the films slightly above $T_P$ and above $T_C$, respectively.

Reppy [5]. The only difference is that the fluid and liquid phases are separated by the solidification at immediately below $n_i$. We consider that, after the inert layer is completed and the lateral pressure becomes significantly small, the uniform 2D liquid phase appears. This hypothesis is consistent with the fact that the superfluid fraction is almost proportional to $(n - n_i)$.

## IV. SUMMARY

In summary, we studied the structure of inert-layer $^4$He in a 2.8-nm channel of FSM, on the bases of vapor pressure and heat capacity data. We also analyzed the heat capacity of the inert layer according to a model that considers the contribution of localized solid and excited fluid. The results support the viewpoint that the excited fluid coexists with the localized solid at high temperatures. With increasing areal density, the amount of excited fluid decreases and tends to zero just below $n_i(\sim n_C)$, suggesting that the inert layer is solidified at values slightly below $n_i$.

## ACKNOWLEDGMENTS

The work was partially supported by JSPS KAKENHI Grants No. JP26400352 and No. JP18K03535. We thank S. Inagaki for supplying FSM.

[1] D. J. Bishop and J. D. Reppy, Phys. Rev. Lett. **40**, 1727 (1978).
[2] G. Zimmerli, G. Mistura, and M. H. W. Chan, Phys. Rev. Lett. **68**, 60 (1992).
[3] M. Shick, in *Phase Transitions in Surface Films*, edited by J. G. Dash and J. Ruvalds (Plenum, New York, 1980).
[4] D. S. Greywall and P. A. Busch, Phys. Rev. Lett. **67**, 3535 (1991); D. S. Greywall, Phys. Rev. B **47**, 309 (1993).
[5] R. H. Tait and J. D. Reppy, Phys. Rev. B **20**, 997 (1979).
[6] R. Toda, M. Hieda, T. Matsusita, and N. Wada, J. Phys.: Conf. Ser. **150**, 032112 (2009).
[7] A. F. Andreev, Pis'ma Zh. Éksp. Teor. Fiz. **28**, 603 (1978) [JETP Lett. **28**, 556 (1978)].
[8] M. Rossi, D. E. Galli, and L. Reatto, J. Low Temp. Phys. **146**, 95 (2007).
[9] S. Inagaki, Y. Fukushima, and K. Kuroda, J. Chem. Soc. Chem. Commun. **22**, 680 (1993).
[10] S. Inagaki, A. Koiwai, N. Suzuki, Y. Fukushima, and K. Kuroda, Bull. Chem. Soc. Jpn. **69**, 1449 (1996).
[11] J. Taniguchi, R. Fujii, and M. Suzuki, Phys. Rev. B **84**, 134511 (2011).
[12] The nitrogen vapor pressure isotherms taken in the previous [11] and the present heat capacity measurements are scaled by areal density and show a plateau at the same pressure due to the capillary condensation. The fact indicates that although a part of channels are blocked, the remaining channels keep the adsorption property of FSM16. A similar decrease of the surface area was observed after the sintering process of the pellet by mixing Ag powder. A creep of Ag powder since the previous measurements may be the origin of blocking the channel.
[13] K. Demura, J. Taniguchi, and M. Suzuki, J. Phys. Soc. Jpn. **86**, 114601 (2017).
[14] J. Taniguchi, K. Demura, and M. Suzuki, Phys. Rev. B **88**, 014502 (2013).
[15] H. Ikegami, T. Okuno, Y. Yamato, J. Taniguchi, N. Wada, S. Inagaki, and Y. Fukushima, Phys. Rev. B **68**, 092501 (2003).
[16] Although the lot number for the 2.8-nm sample is different in the work of Ikegami *et al.* [15] and the present one, the areal density dependences of $\kappa_T$ basically agree with each other.
[17] N. N. Roy and G. D. Halsey, J. Low Temp. Phys. **4**, 231 (1971).
[18] M. Bretz, J. G. Dash, D. C. Hickernell, E. O. McLean, and O. E. Vilches, Phys. Rev. A **8**, 1589 (1973).
[19] J. Daunt, Phys. Lett. A **41**, 223 (1972).
[20] R. Toda, M. Hieda, T. Matsushita, N. Wada, J. Taniguchi, H. Ikegami, S. Inagaki, and Y. Fukushima, Phys. Rev. Lett. **99**, 255301 (2007).